doi:10.26443/seismica.v5i1.2648

Paleoseismology of the Buffalo Valley, Buena Vista, and southern Shoshone faults, central Basin and Range, Nevada, USA

Rich D. Koehler *[1], **Mark W. Stirling** [2], **Brad Sion** [3]

[1]Nevada Bureau of Mines and Geology, University of Nevada, Reno, Reno, NV, USA, [2]Department of Geology, University of Otago, Dunedin, New Zealand, [3]Division of Earth and Ecosystem Sciences, Desert Research Institute, Reno, NV, USA

Author contributions: *Conceptualization*: R. Koehler, M. Stirling. *Funding acquisition*: R. Koehler, M. Stirling. *Investigation*: R. Koehler, M. Stirling. *Formal Analysis*: B. Sion, M. Stirling, R. Koehler. *Visualization*: R. Koehler, M. Stirling. *Writing – original draft*: R. Koehler, M. Stirling. *Writing – review & editing*: all authors. *Project administration*: R. Koehler, M. Stirling.

Abstract We present the results of a study of the Buffalo Valley, Buena Vista, and southern Shoshone faults in central Nevada. The three active normal faults accommodate extension within the slowly deforming Basin and Range Province in central Nevada. For the Buffalo Valley fault, field and lidar observations indicate that deformation is distributed across several parallel strands that progressively displace alluvial fans. Fault trace mapping, vertical displacement estimates, soil pit descriptions from displaced surfaces, and ^{36}Cl exposure age dates from two soil profiles and a single boulder are used to characterise the geomorphology and slip rate of the fault. Cumulative displacement across the oldest surface is ~21 m and late Pleistocene surfaces are displaced 8–8.6 m. Soils developed into late Pleistocene surfaces have stage II+ to III carbonate development suggesting an age for surface stabilization ~60-200 ka. ^{36}Cl soil depth profile analyses refine the age of these surfaces at a minimum of 54 +4/-2 ka and possibly up to 118 ±18 ka where the vertical displacement is 8 m, and a minimum of 77 +5/-1 ka and possibly up to 213 +7/-11 ka where the displacement is 8.6 m, which collectively suggest a vertical slip rate of 0.04–0.15 mm/yr. We further estimate a magnitude of Mw 7.0–7.1 for rupture of the full length of the Buffalo Valley fault from empirical scaling relationships. The Buena Vista and southern Shoshone faults were mapped at single sites where faulted fan surfaces were observed, and boulders were sampled for ^{10}Be exposure age dating. Slip rates of 0.02–0.09 mm/yr and 0.02–0.08 mm/yr for the Buena Vista and southern Shoshone faults, respectively, are estimated from scarp heights and correlation of fan surfaces to Buffalo Valley, and consideration of boulder ^{10}Be exposure ages. The results contribute towards the refinement of seismic hazard models and the assessment of geothermal systems in the region.

Non-technical summary The Buffalo Valley, Buena Vista, and southern Shoshone faults in central Nevada are active faults that accommodate crustal extension in the Basin and Range Province. Geologic mapping, fault scarp profiles, soil descriptions, and cosmogenic exposure dating are used to place constraints on the slip rate of each fault. The results indicate that all three faults have slip rates <0.15 mm/yr. These data are applicable to seismic hazard assessments and regional geothermal resource modeling.

Production Editor:
Andrea Llenos
Handling Editor:
Randolph Williams
Copy & Layout Editor:
Hannah F. Mark

Received:
February 9, 2026
Accepted:
May 13, 2026
Published:
June 1, 2026

1 Introduction

The three active faults addressed in this study are located in the central Basin and Range Province, Nevada USA. The Buffalo Valley fault is an east-dipping normal fault that extends for ~38 km along the east side of the Tobin Range (Fig. 1), while the Buena Vista and Shoshone faults are both west-dipping faults with lengths of ~65 km that bound the eastern Buena Vista Valley and the western Shoshone Range, respectively. The Tobin Range represents a horst structure bound on its west side by the Pleasant Valley fault zone, the source of the 1915 Ms 7.6 Pleasant Valley earthquake (Wallace et al., 1984). Although none of these faults have generated a historic earthquake, long-term tectonic activity is evidenced by prominent tectonic geomorphology including abundant fault scarps crossing alluvial fan surfaces, well-developed triangular facets, and over-steepened basal slopes along their respective range fronts.

Contemporary extensional strain accumulation measured geodetically across the central Basin and Range is ~1 mm/yr (Hammond et al., 2014). This rate largely agrees with cumulative rates of strain release by active faulting determined in several paleoseismic transects across the region (Personius et al., 2017; Wesnousky et al., 2005; Koehler and Wesnousky, 2011). Although the faults in our study occur within the general area of these transects, they have not previously been the subject of detailed slip rate or paleoseismic studies.

Slip rates are important input parameters for constraining deformation models, such as the 2023 update of the U.S. National Seismic Hazard Model (NSHM;

*Corresponding author: rkoehler@unr.edu

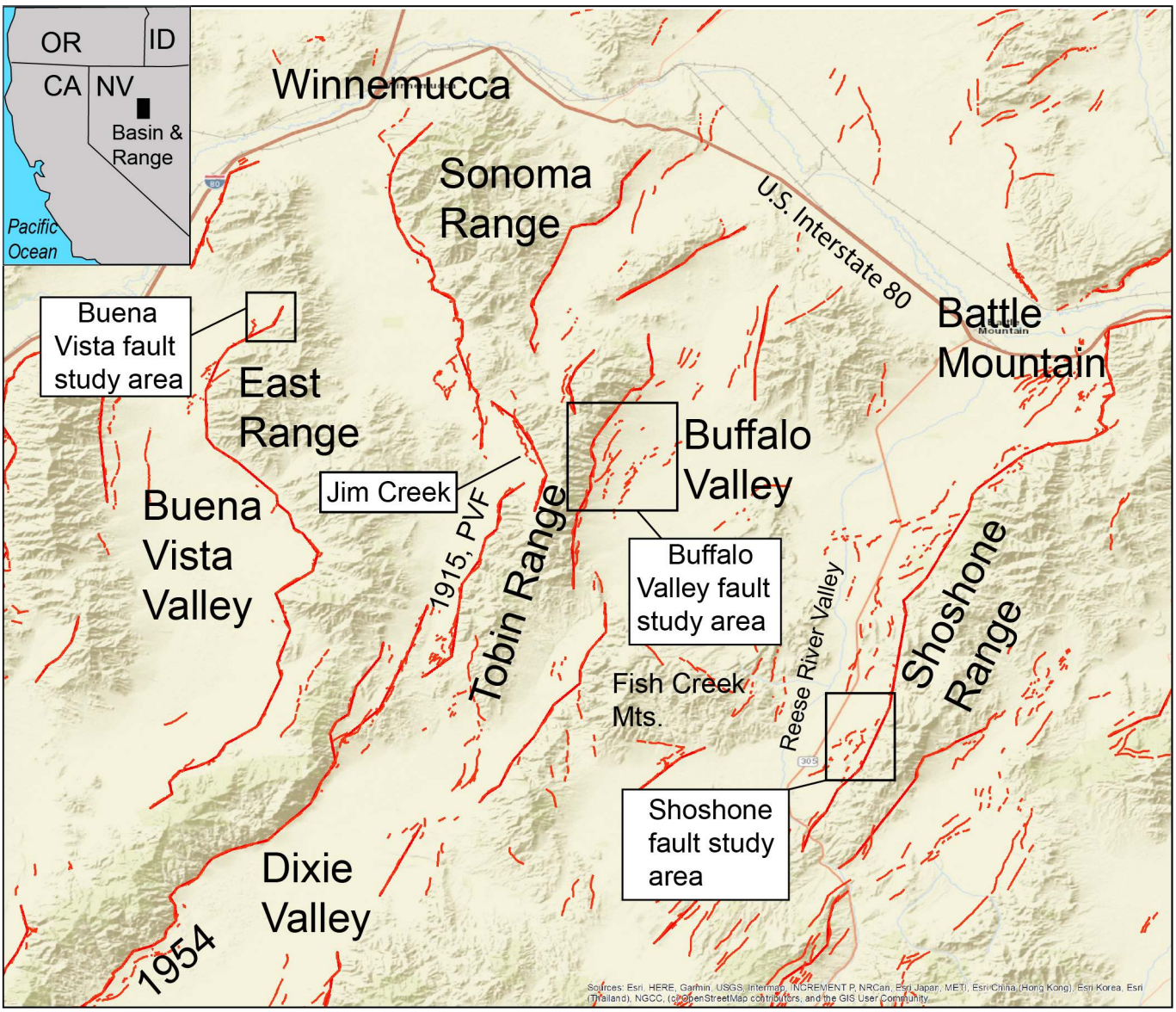

Figure 1 Fault map of central Nevada showing physiographic features and location of the three study areas (labelled). 1954, M6.8 Dixie Valley rupture; 1915, M7.6 Pleasant Valley rupture; PVF, Pleasant Valley fault. Faults from U.S. Geological Survey fault and fold database.

Petersen et al., 2024; Hatem et al., 2022a) and local probabilistic seismic hazards analyses (PSHAs; Valentini et al., 2019). The NSHM assigns a preferred slip rate of 0.1 mm/yr to the three faults; however, these rates were based on evaluation of a suite of uncertainty distributions derived from broad slip rate categories benchmarked by geodetic strain rates (Hatem et al., 2022b) due to lack of geologic observations.

Slip rate and recency of faulting are also important modelling input parameters for assessing potential geothermal energy exploration targets. Specifically, these parameters when combined with other geophysical datasets (e.g. Play-fairway analysis) can inform the potential occurrence of blind geothermal systems (Ayling et al., 2022; Faulds et al., 2016). For example, the intersection of the Buffalo Valley fault with the Jersey Valley fault to the south has been characterized as a structural accommodation zone, a favorable structural setting for potential geothermal energy exploration (Faulds et al., 2021; Burgess and Faulds, 2023).

Motivated by a need to refine the geologic slip rates for the three faults for seismic hazard and geothermal energy applications, we conducted office and field based fault trace mapping on lidar-derived hillshade base maps (USGS, 2023), produced topographic profiles across faulted deposits to assess the amount of displacement, and described and sampled soil pits excavated on the footwall of the Buffalo Valley fault to evaluate the relative and absolute ages of displaced surfaces. We also sampled boulders on faulted fan surfaces on the Buena Vista and Shoshone faults to obtain cosmogenic exposure ages.

2 Observations

2.1 Buffalo Valley fault

The Buffalo Valley fault shows prominent fault scarps and triangular facets along the length of the Tobin Range (Fig. 2). Our mapping efforts focused on a ~7-km-

long section of the fault between Morning View Canyon and Hoffman Canyon where it projects away from the range front and is expressed by multiple subparallel scarps and grabens that displace alluvial fans of various ages (Fig. 3A). Fault traces and Quaternary alluvial fans were mapped using lidar-derived hillshades and field reconnaissance. Alluvial fan units were differentiated primarily based on cross cutting and inset relations, relative degree of incision, and drainage patterns. The units include relatively old (Qfo), intermediate (Qfi), and young (Qfy) alluvial fans, following common stratigraphic nomenclature in the Basin and Range (e.g. Koehler and Wesnousky, 2011). The distribution of these surfaces is shown on Fig. 3B. In general, Qfo alluvial surfaces are characterized by deep gully dissection and rounded interfluves. Qfi alluvial surfaces are characterized by relatively flat surfaces with moderate gully dissection that are inset into Qfo deposits. Qfy deposits are confined to active channels deeply eroded (12-20 m) into Qfo and Qfi deposits in upslope areas and spread out across the piedmont downslope of the fault where they are characterized by anastomosing distributary channels.

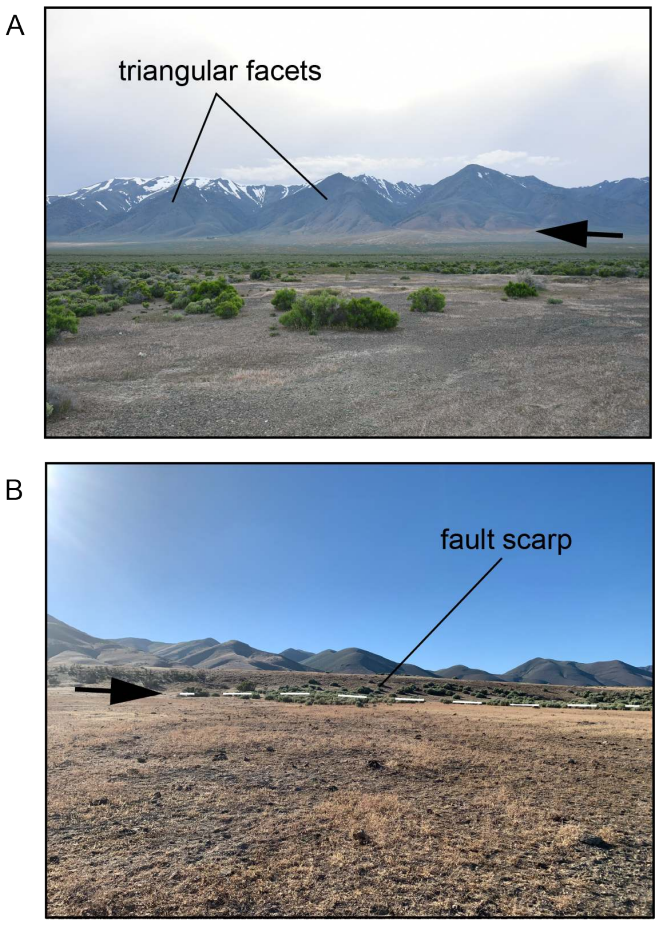

Figure 2 Field photographs showing: (A) prominent tectonic geomorphology along the southern Buffalo Valley fault range front; and (B) a ~5-m-high scarp extending across an alluvial fan at the location of soil pit BVSP-2 (See Fig. 3B for location). Black arrow points to fault in both images. Dashed white line indicates base of scarp in (B).

A pluvial lake existed in Buffalo Valley in the late Pleistocene (Mifflin and Wheat, 1979; Reheis, 1999). Al-

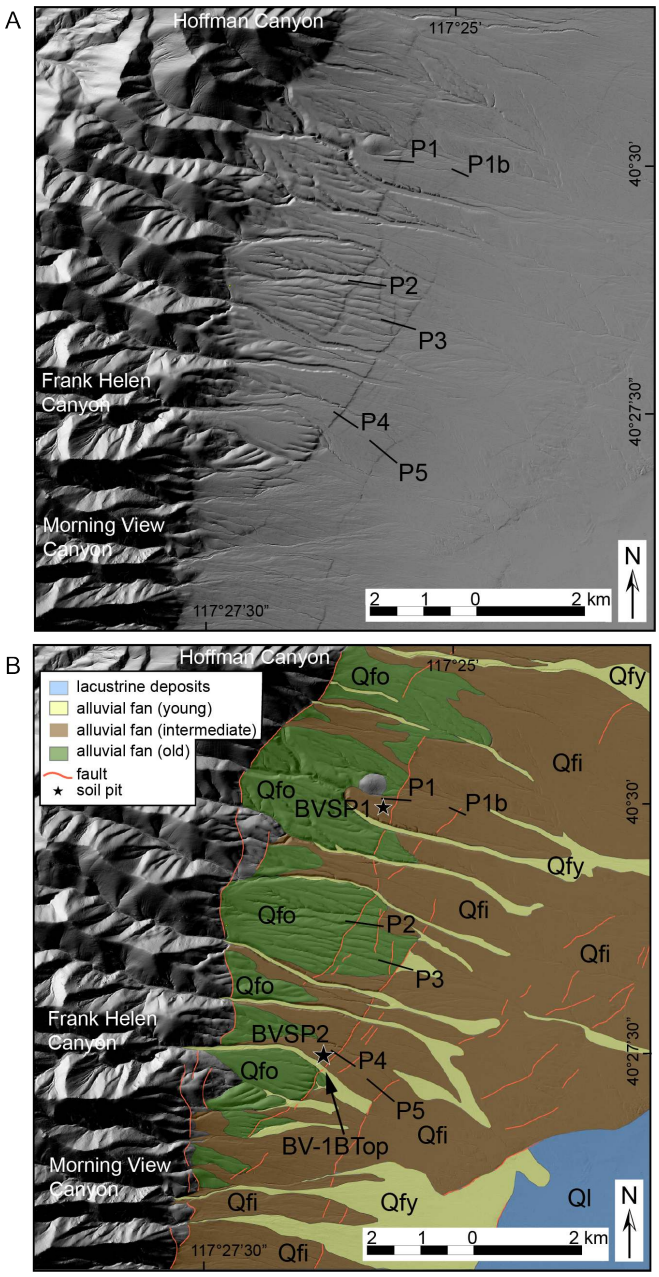

Figure 3 Buffalo Valley study area. (A) uninterpreted lidar hillshade of the Buffalo Valley fault; and (B) Quaternary geologic map of the Buffalo Valley fault. Black stars show locations of soil pits. Black lines indicate locations of scarp profiles shown in Fig. 4. Lidar hillshade base maps in both panels from USGS (2023), 1-m resolution.

though undated, Mifflin and Wheat (1979) inferred that the lake existed during the time of pluvial Lake Lahontan which dessicated after ~15.5 cal. YBP (Adams and Wesnousky, 1999; Adams et al., 2008). The lake reached a maximum elevation of ~1,412–1,416 m based on the sill elevation at the eastern side of the valley. This elevation is lower than the majority of mapped fault scarps, providing confidence that they are tectonic in origin, and not shoreline features. However, field inspection of subtle scarps near the late Pleistocene highstand elevation along the western margin of the basin revealed that these scarps have rounded crests and curvilinear topographic forms consistent with constructional beach berm features. In several cases, mapped faults project

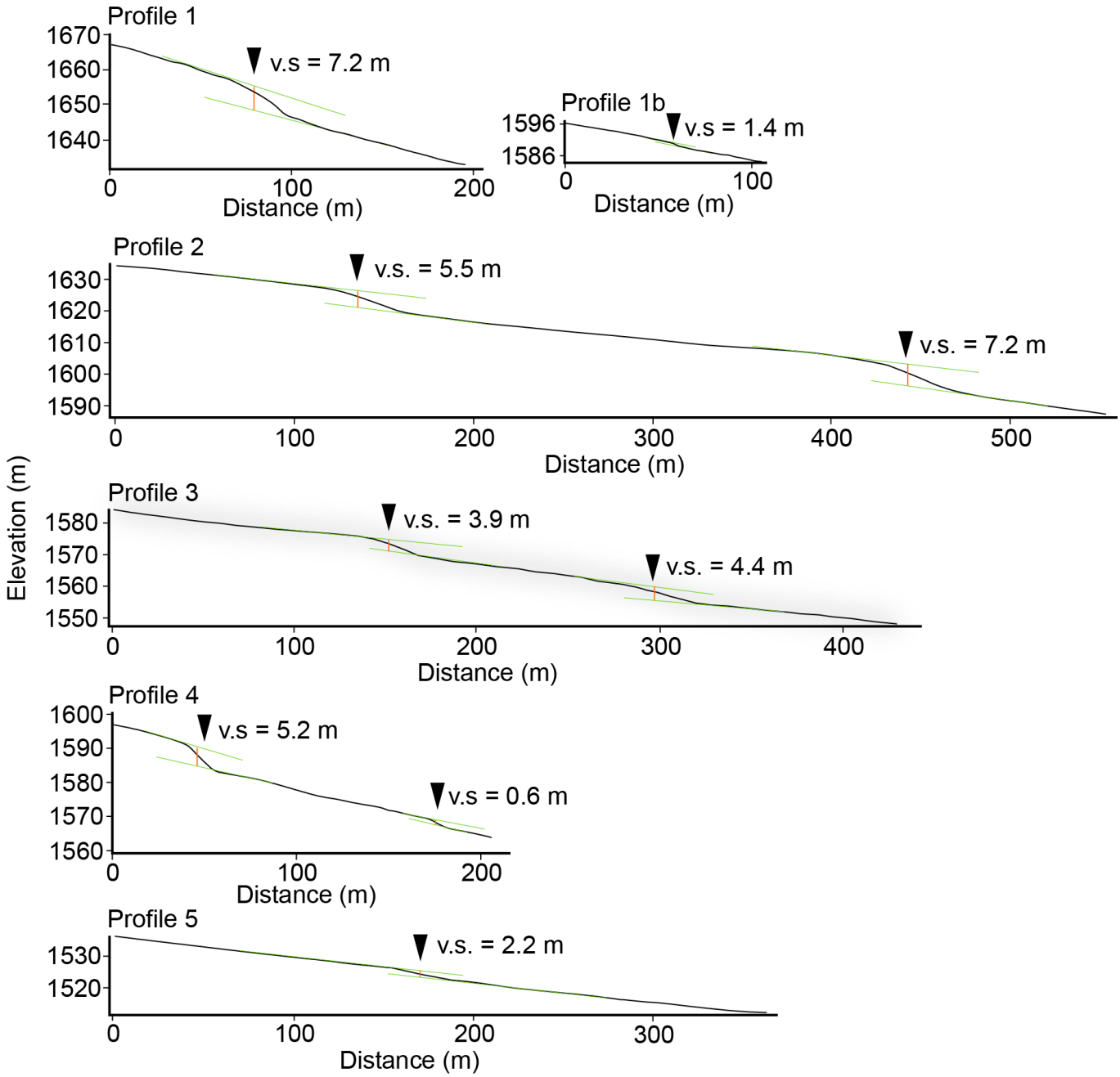

Figure 4 Topographic profiles surveyed across fault scarps that displace middle Pleistocene Qfo fans (Profiles 2 and 3: BVSP-1) and late Pleistocene Qfi fans (Profiles 1, 1b, 4, and 5: BVSP-2) along the Buffalo Valley fault. Light green lines indicate slope projections used to estimate vertical separation. Profile locations are shown on Figure 3B. Along each profile black arrow indicates location of fault interpreted from lidar data. Vertical exaggeration (2x) in all profiles.

into shoreline features (Figure 3B, southeastern corner) indicating that some lower elevation scarps are tectonic in origin but have been modified by lacustrine processes.

Soil pits were excavated to a depth of 2 m on the footwall alluvial surfaces of two displaced intermediate age (Qfi) alluvial fans (Figs. 3, 5, and 6). Characteristics of individual soil horizons exposed in the pits were described including color, structure, consistency, and texture (Supplemental Section S1). The degree of carbonate accumulation ($CaCO_3$ stage) was assessed to evaluate the relative age of surface abandonment. Bulk sediment samples were collected at 25 cm intervals (beginning at 20 cm depth) from each pit for ^{36}Cl depth profile analysis to assess the numeric age of the soil/surface. A complete lab report detailing the geochronologic methods and results is provided in Supplemental Section S2.

The soil exposed in soil pit BVSP-1 (GPS coordinates 40.5006°, -117.4276°) is characterized by a 20-cm-thick sandy clay loam textural Btb horizon and an 80-cm-thick loamy sand Bkb horizon with stage II+ to III carbonate development. The soil exposed in soil pit BVSP-2 (GPS coordinates 40.4580°, -117.4381°) near Frank Helen Canyon is characterized by a 20-cm-thick Btb horizon with a silty clay loam texture and a 45-cm-thick silty clay to clay Btkb horizon with Stage II+ carbonate development. The textural B horizons in both pits are overlain by silt loam to sandy loam A and Bw hori-

zons with weak structure (22 cm thick in BVSP-1 and 13 cm thick in BVSP-2). This relation suggests Holocene erosion, deposition, and subsequent soil development on an older late Pleistocene surface, a phenomenon widely observed in the Great Basin in Nevada (Machette et al., 2005; Adams and Wesnousky, 1999; Koehler and Wesnousky, 2011). Both pits have relatively thick textural Btb and Bkb horizons suggesting relative antiquity; however, the soil in pit BVSP-2 has slightly less carbonate development. Based on the degree of carbonate development (Stage II+ – III) and comparison to regional datasets (Eppes et al., 2003; Harden et al., 1985; Redwine et al., 2021; Machette, 1985) we were initially able to infer that the alluvial surfaces were abandoned and soil began to form in the late middle to late Pleistocene about 60–200 ka. This broad age range is consistent with regional patterns of fan aggradation that occurred in climatic transitions between Marine Oxygen Isotope stages 4–3 (~70 ka) and 6–5 (~130 ka; Eppes et al., 2003).

^{36}Cl depth profile exposure ages place additional constraints on the age of the alluvial surfaces. Because of potential soil disturbance and/or burial of the late Pleistocene soil by a Holocene soil as observed in the soil pits, the samples from the AB/Bw horizon in BVSP-1 and Av/Bw horizon and the top of the 2Btb horizon in BVSP-2 complicated the age modelling. Thus, age models were evaluated in two separate ways for each pit: first including all depth samples, and second using only samples below 50 cm (Supplemental Section S3). Using all samples from the depth profile, the profile age for soil pit BVSP-1 is 77 +5/-1 ka, and soil pit BVSP-2 shows an age of 54 +4/-2 ka. Excluding samples from the upper 50 cm of the profiles results in a modelled age of 202–220 ka (213 ka mean Bayesian solution) for soil pit BVSP-1 and 100–136 ka (118 ka mean Bayesian solution) for soil pit BVSP-2. The Bayesian solution is the method used to solve the best fitting depth profile (Marrero et al., 2016). The age difference for the two profiles is considerable, despite both being mapped as Qfi alluvial surfaces. The deeper incision of drainage systems at soil pit BVSP-1 is consistent with Qfi being older there than at soil pit BVSP-2 and implies a reasonably broad age range represented by Qfi deposits. Thus, we apply a range of 52–220 ka for the Qfi fans, consistent with the ages inferred from soil carbonate stage development.

We also sampled a single boulder (sample BV-1B Top) on a Qfy surface on the footwall of a < 1 m fault scarp immediately south of soil pit BVSP-2 (Fig. 3; Supplementary Section S4) for ^{10}Be exposure age dating. The exposure age of 45 ± 4 ka (Supplemental Section S5) is reasonable, given that it is the youngest surface above the active channel floodplain and inset to the Qfi surface at BVSP-2.

Topographic profiles were extracted from lidar point cloud data orthogonal to fault scarps that displace Qfo and Qfi alluvial surfaces and used to measure vertical separation across the scarps (Figs. 3 and 4). Profiles 1 and 1b extend across two scarps in the vicinity of soil pit BVSP-1 and indicate a vertical separation of 8.6 m of the Qfi surface. Profiles 2 and 3 extend across multiple sub parallel scarps that displace a Qfo surface and indicate a cumulative vertical separation of 21 m. Profiles 4 and 5 extend across three parallel scarps in a Qfi surface near soil pit BVSP-2 and indicate a cumulative vertical separation of 8 m. The cumulative displacements are considered a minimum because an unknown amount of displacement may be accommodated along the range front, and subtle scarps outside the limits of the profiles may exist.

We calculate a late Pleistocene vertical slip rate for the Buffalo Valley fault by dividing the cumulative displacement of the Qfi surface (three traces) at soil pit BVSP-2 (8 m) by the range of ages obtained from the ^{36}Cl cosmogenic exposure dating of the soil developed into the faulted surface (52–136 ka). The resulting vertical slip rate is 0.06–0.15 mm/yr. Similarly, a slip rate of 0.04–0.11 mm/yr is calculated from the cumulative displacement of Qfi at soil pit BVSP-1 (8.6 m) and the range of cosmogenic exposure ages for the soil profile (76–220 ka). These results collectively give a slip rate range of 0.04–0.15 mm/yr, which we consider to be a minimum estimate for the fault based on the unknown amount of slip at the range front and slip on undetectable scarps to the east of the profiles.

In the above calculations of slip rate, we favor use of the relatively older Qfi surface because of the consistency of soil profile-based exposure age estimates, and its association with multiple-event scarps. We do not use the single cosmogenic ^{10}Be exposure age obtained from the boulder sample on the Qfy surface (Fig. 3). Although the age of the boulder is reasonable, the small size of the scarp suggests that it is the result of a single event. Additionally, small channels on the surface suggest overtopping of the active channel by floods, which could have modified the position of the boulder. Despite these uncertainties, the boulder age of 45 ka may represent the elapsed time since the most recent earthquake along the Buffalo Valley fault.

2.2 Buena Vista fault

Our study of the Buena Vista fault focused on the Willow Creek area at the northern end (Fig. 7). Our mapping of the site uses the same nomenclature as for the Buffalo Valley fault and shows prominent scarps displacing late Pleistocene (Qfi) alluvial surfaces, and two late to middle Pleistocene alluvial surfaces (Qfo1 and Qfo2). The subdivision of Qfo was necessary because of inset relations and differences in fan geomorphology. Vertical separation across the scarp in Qfi deposits ranges from 1.5 m (Profile 6) adjacent to Willow Creek and 4.9 m (Profile 9) approximately 2 km southwest of Willow Creek (Figs. 7 and 8). Where the fault displaces the Qfo2 surface the hanging wall is buried by Qfo1 and Qfi deposits within a complex graben (Fig. 7). The vertical separation across the Qfo2 surface is 14.5 m (Profiles 7 and 8, Figs. 7 and 8) but may be less given the position of the graben west of the main scarp.

The morphology of the Qfi fans along the Buena Vista fault is similar to the Buffalo Valley fans, from which we infer that they have a similar relative age (52–220 ka). Cosmogenic ^{10}Be exposure ages for three boulders on the displaced Qfi surface adjacent to Willow Creek are 699 ± 85 ka, 167 ± 15 ka, and 178 ± 16 ka (samples BVN-

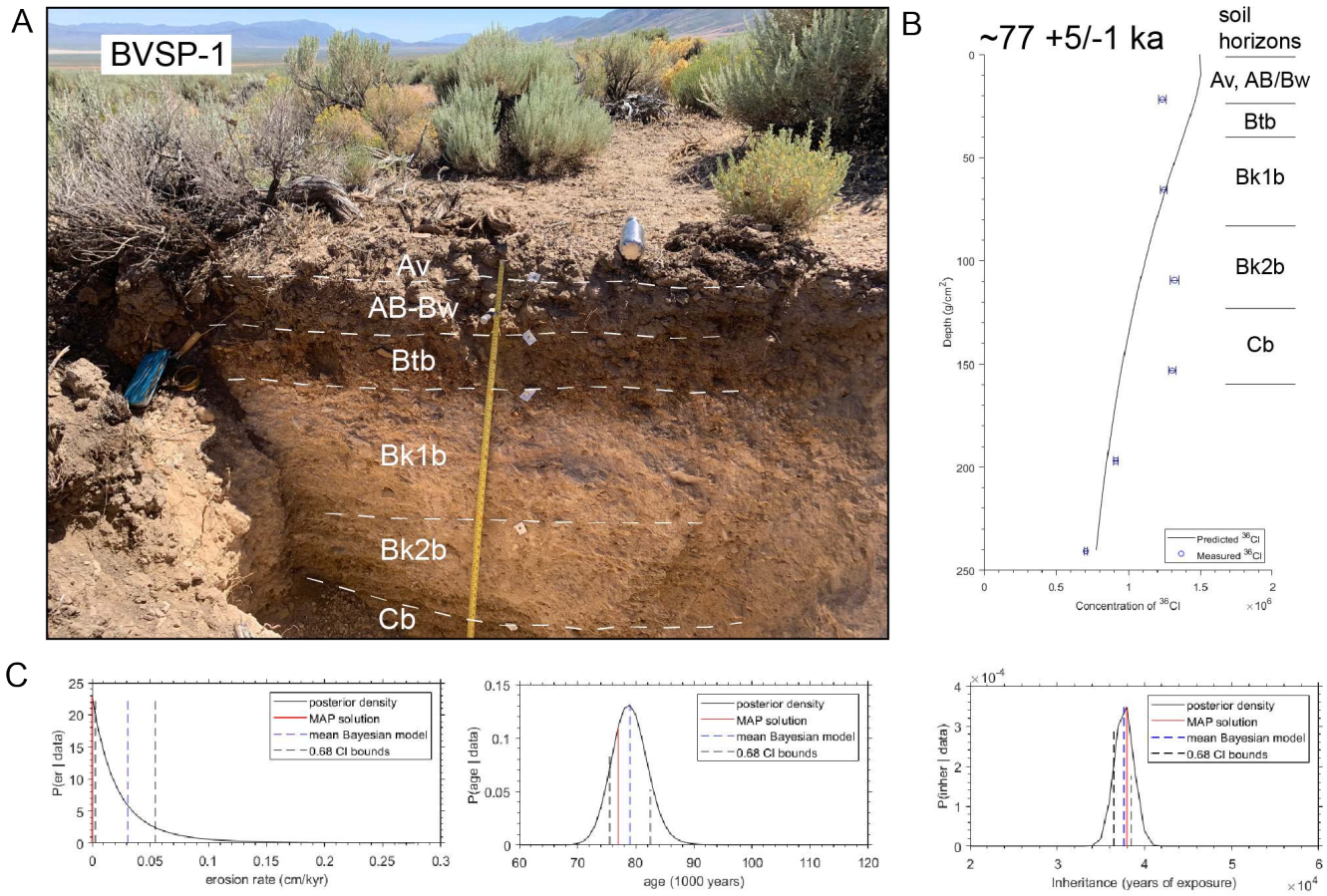

Figure 5 Soil pit BVSP-1. (A) Photograph of soil pit exposure with soil horizons designated, (B) ^{36}Cl concentration and soil horizons versus depth, and (C) from left to right probability distributions of density, age, and inheritance that correspond to model fits to the ^{36}Cl depth profile in B. The best fitting curve shown in B corresponds to an age ~77 +5/-1 ka.

01, BVN-02, and BVN-03, respectively; Fig. 7 and Supplementary Sections S4 and S5). While sample BVN-01 is clearly older than our inferred 52–220 ka age based on correlation to the Qfi alluvial surfaces in Buffalo Valley, the latter two ages (BVN-02 and BVN-03) are compatible. At the location where the boulders were sampled, the scarp is 1.5 m high and has a smooth, unbevelled profile, suggesting that it is the result of a single event. This implies that only one earthquake has occurred in 167–178 ka, a very long time period relative to the typical recurrence intervals of Basin and Range faults (e.g. Wesnousky et al., 2005). The 699 ka exposure age (sample BVN-01) appears to have been influenced by inheritance because the age is much older than the other two samples from the same surface. We suspect that the boulder may have been derived from a much older surface further up catchment or eroded off the adjacent Qfo surface and has inherited additional ^{36}Cl isotope concentrations while exposed. In consideration of these ambiguities we do not use the scarp height observations and boulder exposure ages adjacent to Willow Creek in the determination of slip rate. We calculate a late Pleistocene vertical slip rate of 0.02–0.09 mm/yr for the Buena Vista fault based on the scarp height of the displaced Qfi fan surface 2 km southwest of Willow Creek (4.9 m vertical displacement at Profile 9; Fig. 8), and assuming that the exposure ages for displaced Qfi alluvial surfaces along the Buffalo Valley fault (52–220 ka) are a reasonable approximation for the age of the Qfi alluvial surfaces along the Buena Vista fault.

2.3 Southern Shoshone fault

Our study of the southern Shoshone fault focused on the mouth of an unnamed drainage within the area shown in Figure 1 in southern Reese River Valley (Valley of the Moon). The site shows prominent scarps displacing a late Pleistocene (Qfi) alluvial surface, and two late to middle Pleistocene (Qfo1 and Qfo2) alluvial surfaces (Fig. 9). The Qfi alluvial surface has similar surficial characteristics to the Qfi fans exposed along the Buffalo Valley and Buena Vista faults from which we infer it has a similar relative age (52–220 ka).

We calculate a late Pleistocene vertical slip rate of 0.02–0.08 mm/yr for the southern Shoshone fault based on the total displacement of the Qfi surface across two fault strands (combined 4.5 m vertical separation, Profiles 11 and 11b; Figs. 9 and 10), and using the exposure ages for Qfi alluvial surfaces in Buffalo Valley (52–220 ka) with the assumption that the similar fan morphology in both valleys indicates a similar age. ^{10}Be exposure ages taken from a boulder on the Qfi surface is 262 ± 24 ka (sample SHS-06), and ages of 389 ± 39 ka (sample SHS-09) and 726 ± 90 ka (sample SHS-07) are obtained from the Qfo1 surface (Fig. 9 and Supplemental Sections S4 and S5). The Qfi surface exposure age is some-

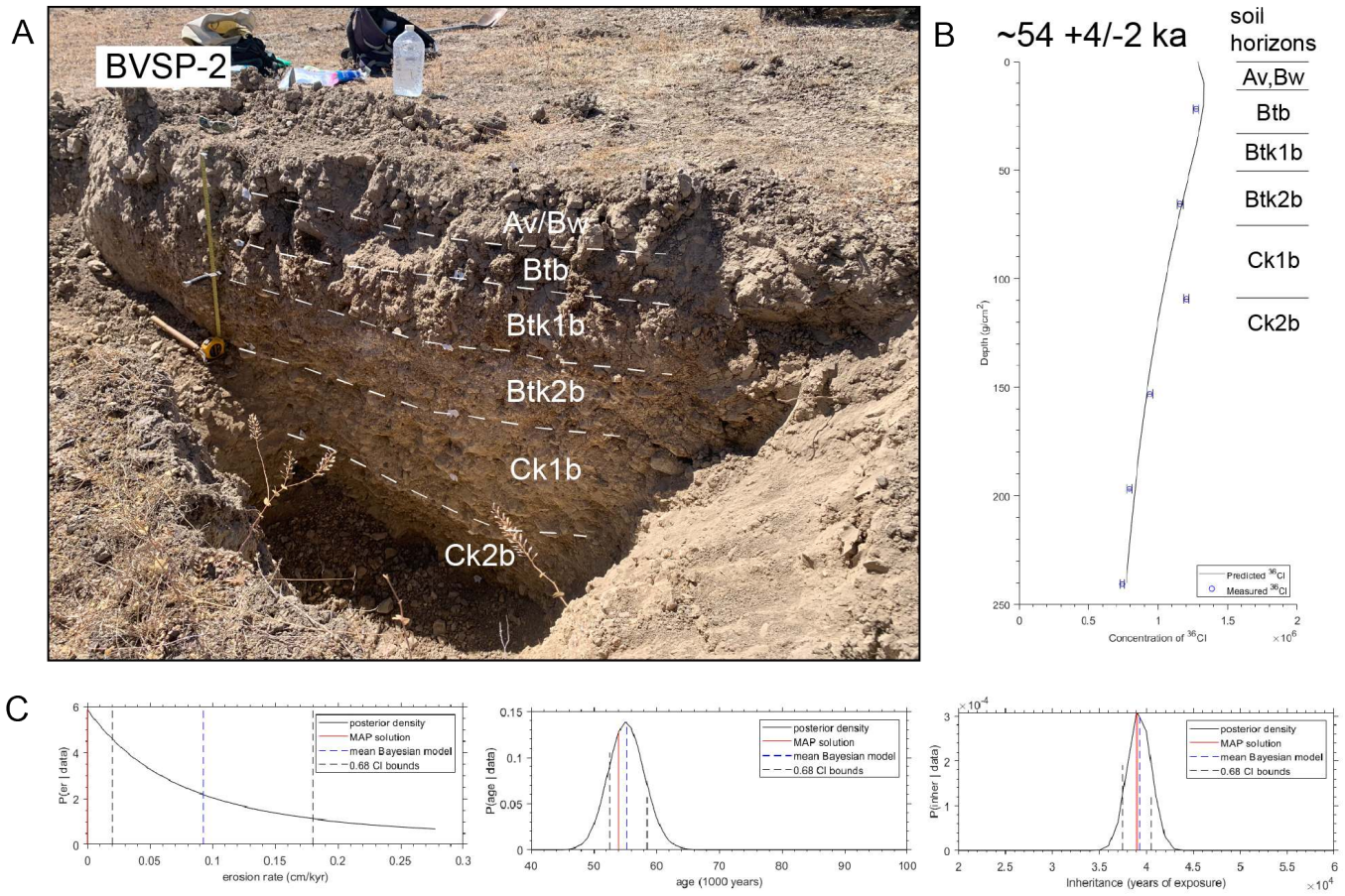

Figure 6 Soil pit BVSP-2. (A) Photograph of soil pit exposure with soil horizons designated, (B) ^{36}Cl concentration and soil horizons versus depth, and (C) from left to right probability distributions of density, age, and inheritance that correspond to model fits to the ^{36}Cl depth profile in B. The best fitting curve shown in B corresponds to an age ~54 +4/-2 ka.

what older than the 52–220 ka we use in the slip rate determination, but the resulting change to the minimum slip rate (0.03 mm/yr) is negligible. The Qfo1 exposure ages are reasonable, given that Qfo alluvial surfaces are generally assumed to be middle Pleistocene in central Nevada (Koehler and Wesnousky, 2011). A slip rate of 0.02–0.03 mm/yr can be estimated using the Qfo1 exposure ages and the vertical separation of 11.2 m (Profile 10, Fig. 10). This rate overlaps with the lower end of the rate determined from the Qfi surface.

3 Discussion

Our mapping, analysis, and interpretations show that the three faults in this study have slip rates within the range of slip rates for central Basin and Range faults. Machette et al. (2005) determined a slip rate for the Clan Alpine fault of 0.025–0.08 mm/yr. For the Fairview Peak fault which ruptured in the 1954 M7.1 Fairview Peak earthquake, Bell et al. (2004) determined a vertical slip rate of 0.04–0.21 mm/yr. Based on soil profiles with stage II+ carbonate development, Koehler and Wesnousky (2011) inferred an age for Qfi alluvial fans displaced by faults across U.S. Highway 50 of around 70–130 ka. Their estimate of fan age was based on regional aggradation patterns that occurred during climatic transitions between Marine Oxygen Isotope stages 4–3 (~70 ka) and 6–5 (~130 ka) described by Eppes et al. (2003) and regional studies of carbonate development in soils (e.g. Machette, 1985). The vertical displacements and ages of faulted deposits reported by Koehler and Wesnousky (2011) allow the interpretation of vertical slip rates for the Toiyabe Range fault (0.03–0.05 mm/yr) and the Butte Range fault (0.04–0.08 mm/yr). Considering the regional fan aggradation patterns (~70–130 ka; Eppes et al., 2003) which overlap with our inferred soil age determinations and numeric ages in Buffalo Valley we prefer slip rates of 0.06–0.12 mm/yr for the Buffalo Valley fault, 0.04–0.07mm/y for the Buena Vista fault, and 0.03–0.06 mm/yr for the Shoshone fault.

In the context of recurrence intervals, the slip rates determined in this study for the three faults combined with an assumed vertical displacement of 1–2 m per event would imply earthquake recurrence intervals of 7–50 ka for the Buffalo Valley fault, 11–100 ka for the Buena Vista fault, and 13–100 ka for the southern Shoshone fault. These are extreme-bound recurrence intervals, combining maximum displacement with minimum slip rate, and vice versa. While these are long recurrence intervals on an individual fault basis, the combined recurrence interval for ground rupturing earthquakes for the three faults is much shorter (3–25 ka).

Estimates of the maximum size of an earthquake that would accompany rupture of the full length of the Buf-

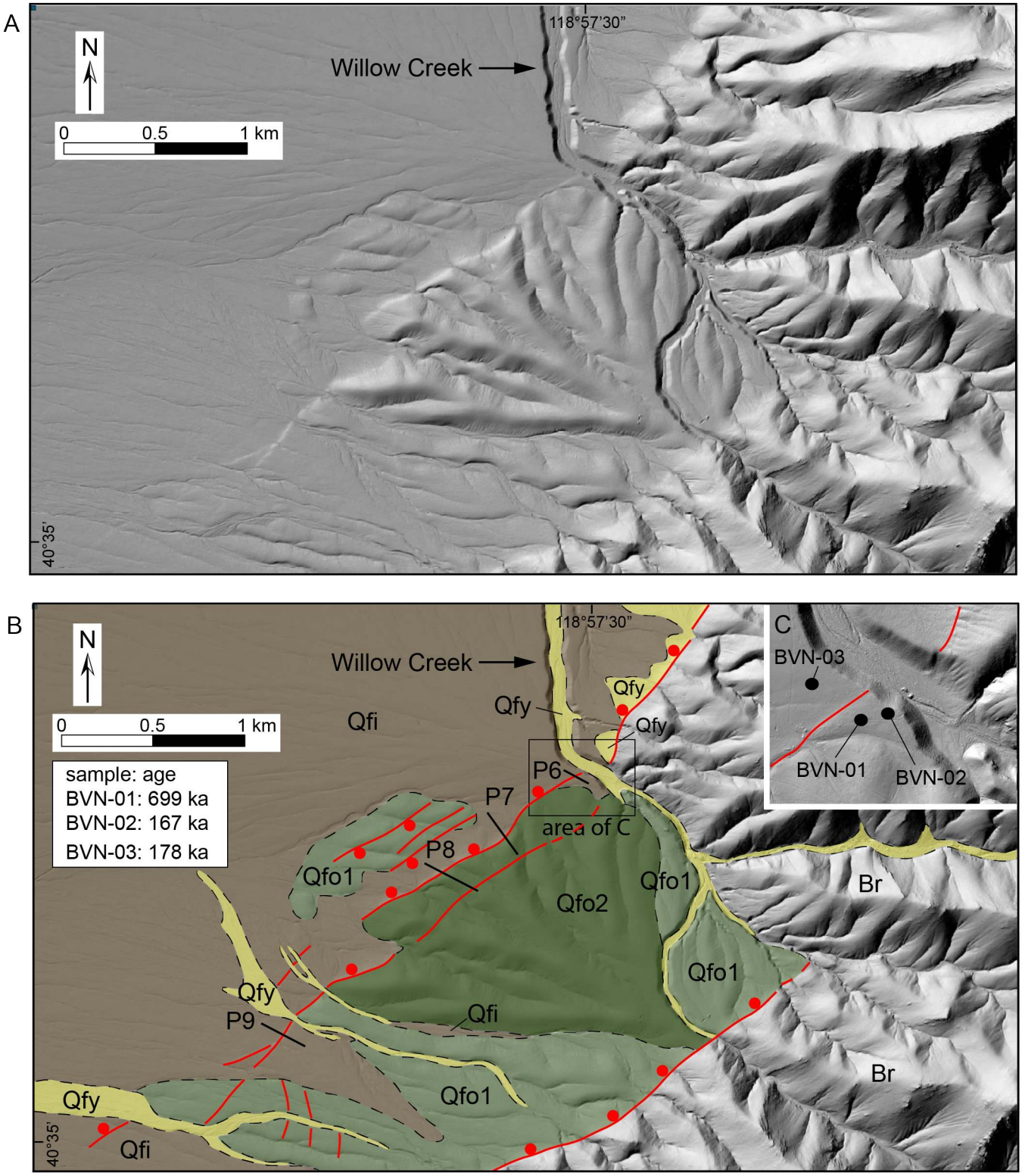

Figure 7 Buena Vista fault study area near Willow Creek (GPS coordinates 40.6051°, -117.9610°). (A) Uninterpreted lidar hillshade of the Buena Vista fault site; and (B) Quaternary geologic map of the site. (C) Enlarged image showing displaced Qfi fan and boulder sample locations for ^{10}Be cosmogenic exposure dating (black circles). Black lines indicate locations of scarp profiles shown in Fig. 8. Lidar hillshade base maps in all panels from US Geological USGS (2023), 1-m resolution.

falo Valley fault can be made using the magnitude-rupture area scaling relations of Stirling et al. (2023). The total rupture length of the fault is supported by geomorphic observations of similar scarp heights along the length of the fault. Using a 38 km fault length, and reasonable estimates of seismogenic thickness (15–20 km) and fault dip (42–45°) for the Basin and Range, an estimate of Mw 7.0 ± 0.2 is obtained for the Buffalo Valley fault. An alternative method for estimating Mw takes account of single event displacement (SED; Hanks and Kanamori, 1979). Assuming single event displacements of ~2 m along the Buffalo Valley fault (similar to the 1915 earthquake on the Pleasant Valley fault; Wallace, 1984) yields a maximum estimate of Mw 7.1. Maxi-

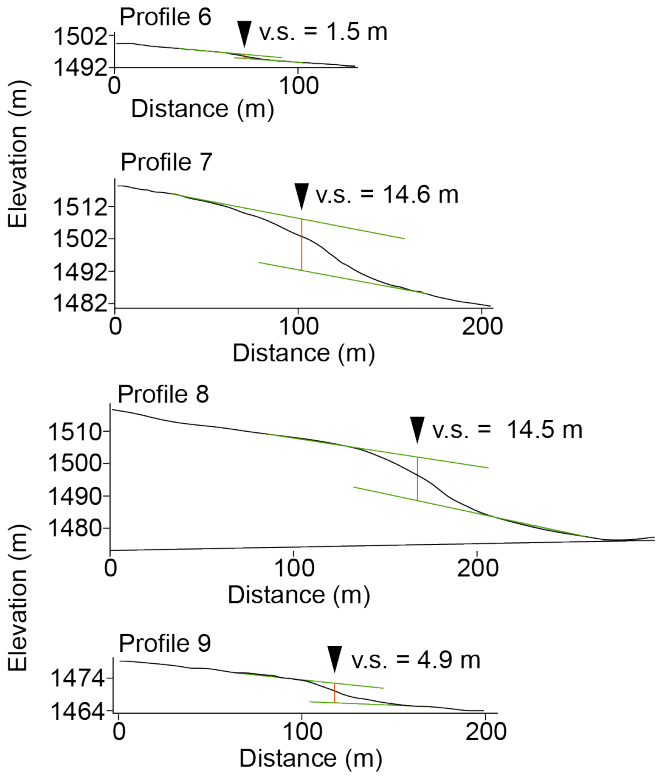

Figure 8 Topographic profiles surveyed across fault scarps that displace middle Pleistocene Qfo fans (Profiles 7 and 8), and late Pleistocene Qfi fans (Profiles 6 and 9) along the Buena Vista fault. Light green lines indicate slope projections used to estimate vertical separation. Note that the scarp heights in Profiles 7 and 8 may under-represent the true throw on Qfo as the hanging wall is mantled with Qfi fan deposits. Along each profile black arrow indicates location of fault interpreted from lidar data. Profile locations are shown on Fig. 7.

mum magnitude was not calculated for the Buena Vista or Shoshone Range faults because of uncertainties related to rupture length and possible segmentation along these long and geometrically complex faults.

Geochronologic studies are relatively few in the central Basin and Range; however, they are becoming more available as the techniques are refined. Geomorphic characteristics and numeric chronologies of alluvial fans from the Walker Lane to the west (e.g., Bormann et al., 2012; Angster et al., 2019) and Pleasant Valley (e.g. Figueiredo et al., 2023, 2024) are similar to the Qfi fans in Buffalo Valley, implying a reasonable relation of Qfi fans across this part of the Basin and Range. Along the Wassuk Range fault, Bormann et al. (2012) report ^{10}Be and ^{26}Al exposure ages on boulders of ~85-125 ka for a Qfi surface displaced 40 m. In a study of the Petrified Springs fault, Angster et al. (2019) applied multiple different dating methods to a Qfi surface with a stage III carbonate soil. The geochronologic results indicate a ^{36}Cl depth profile age of 153 ka and ^{10}Be exposure ages on boulders showed a younger age population (94–165 ka) and an older age population (229–560 ka). Based on the carbonate stage, Angster et al. (2019) preferred the younger population which overlaped with the ^{36}Cl depth profile age. Figueiredo et al. (2023, 2024) conducted geochronologic analyses on alluvial fans along the Pleasant Valley fault along the western flank of the Tobin Range at the latitude of our study. At Jim Creek, they report preliminary ages from four ^{36}Cl depth profiles that range between 56–134 ka (average 90 ka) and calculate a mínimum vertical slip rate of 0.05–0.1 mm/yr based on the combined vertical separation across two strands of the fault of 8.25 m. The alluvial fans studied by Figueiredo et al. (2023, 2024) have similar geomorphic expresion and soil development to the fans we studied in Buffalo Valley, as well as the same bedrock parent materials (Greenstone, chert, and argillite of the Carboniferous Pumpernickel formation and dominantly chert and quartzite of the Permian Havallah formation; Muller et al., 1951). Soil exposures in the Jim Creek alluvial fan observed during our reconnaissance have an ~20 cm A-Bw horizon that buries relatively thick Btb and Btkb horizons, virtually identical in horizonation and thickness to the alluvial fans we studied in Buffalo Valley. Furthermore, the ages and slip rate determined by Figueiredo et al. (2024) to the west of the Tobin Range and our estimates in Buffalo Valley to the east of the range support the notion of the Tobin Range deforming as a horst block bound by the Pleasant Valley and Buffalo Valley faults.

The Buffalo Valley fault shows considerable variation in morphology and complexity along its strike. The central section of the fault is the only section where multiple traces are observed to the east of the Tobin Range front, whereas the fault is confined to the range front to the north and south. The range front facets are also much more developed to the north and south, and the Tobin Range is much higher in these areas. The correlation of the lowest central part of the Tobin Range with the distributed scarps along the Buffalo Valley fault is perhaps a manifestation of the overall development of the range. The range may have commenced development as two separate ranges, but eventually coalesced to form a range with a topographic low in the center. The complex distributed central section of the Buffalo Valley fault may therefore be the least developed section of the fault and may eventually evolve to a more simple range front fault with ongoing cumulative slip. The central section of the fault is also associated with a left step and several traces obliquely oriented to the main fault. These complexities may represent a breached step over or relay ramp, a favorable setting for blind geothermal resources (e.g. Faulds et al., 2021).

4 Conclusions

We have developed slip rate estimates for the Buffalo Valley, Buena Vista, and southern Shoshone faults in central Nevada. Fault trace mapping, vertical separation estimates, soil pit descriptions from displaced alluvial surfaces, ^{36}Cl exposure age dates from two soil profiles, and ^{10}Be exposure ages from alluvial surface boulders were used to characterise the geomorphology and slip rate of the three faults. For the Buffalo Valley fault, ^{36}Cl soil depth profile analyses at two sites on intermediate (Qfi) alluvial fan surfaces give exposure

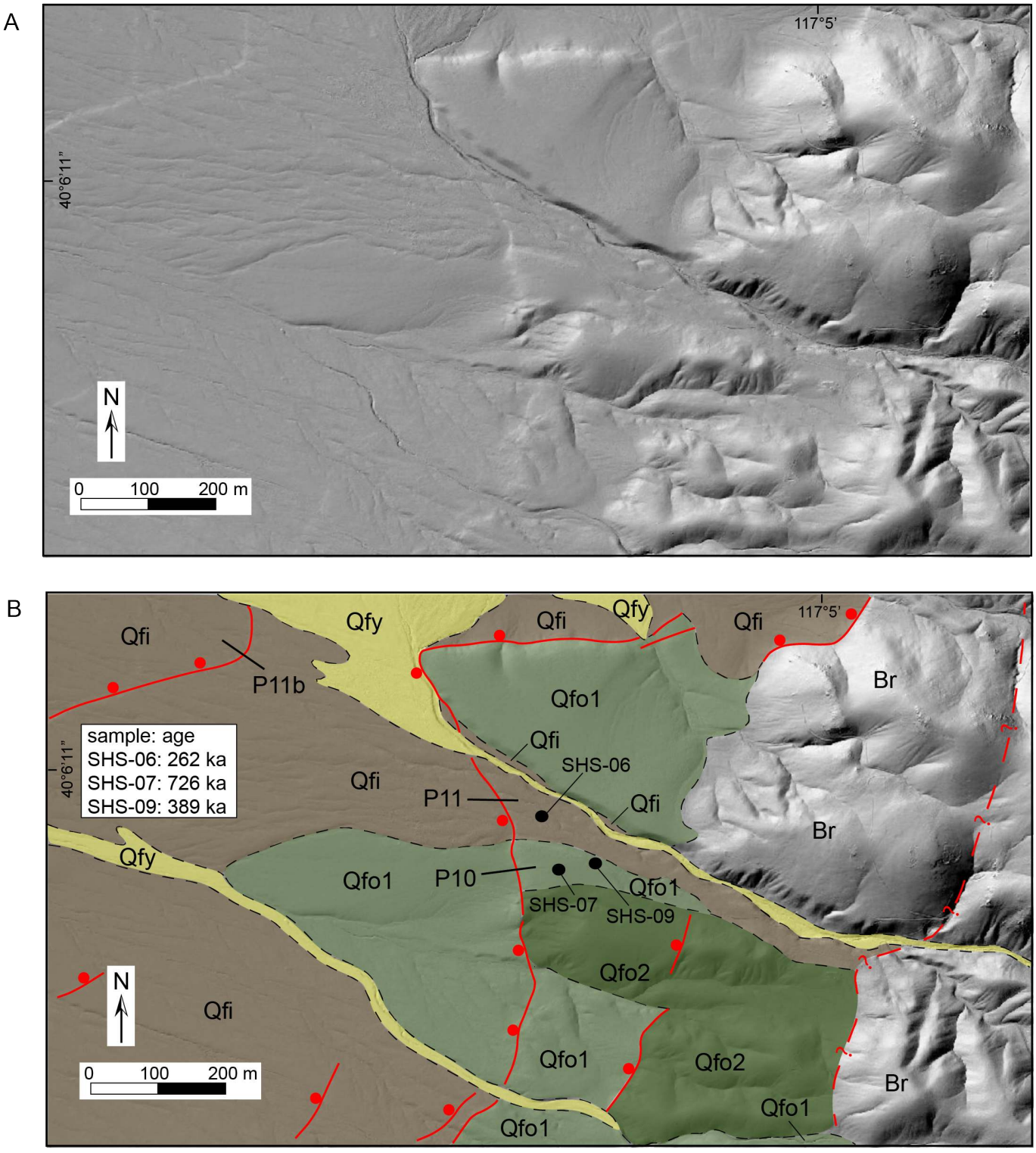

Figure 9 Southern Shoshone fault study area (GPS coordinates 40.1022°, -117.0950°). (A) uninterpreted lidar hillshade of the Southern Shoshone fault site; and (B) Quaternary geologic map of the site. Boulder samples for ^{10}Be cosmogenic exposure dating are shown by black circles. Black lines indicate locations of scarp profiles shown in Fig. 10. Lidar hillshade base maps in both panels from US Geological USGS (2023), 1-m resolution.

age estimates of 52–136 ka where the vertical displacement on the fault is 8 m, and 76–220 ka where the displacement is 8.6 m. These data suggest a vertical slip rate of 0.04–0.15 mm/yr. Magnitude estimates of Mw 7.0–7.1 are made for rupture of the full length of the fault. The Buena Vista and southern Shoshone faults were mapped at single sites where faulted alluvial fan surfaces were observed. Slip rates of 0.02–0.09 mm/yr and 0.02–0.08 mm/yr for the Buena Vista and southern Shoshone faults, respectively, are estimated from scarp heights and correlation of fan surface morphology to Buffalo Valley, and consideration of boulder ^{10}Be exposure ages. The results provide independent geologic validation of slip rates used (~0.1 mm/yr) in the 2023 U.S. National Seismic Hazard Model (Hatem et al., 2022b). This work highlights the importance of utiliz-

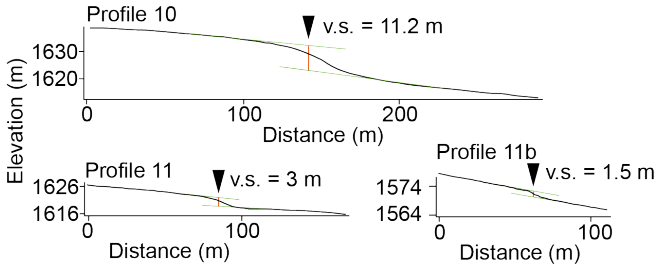

Figure 10 Topographic profiles surveyed across fault scarps that displace a middle Pleistocene Qfo1 fan (Profile 10), and a late Pleistocene Qfi fan (Profiles 11 and 11b) along the southern Shoshone fault. Light green lines indicate slope projections used to estimate vertical separation. Note that the scarp height in Profile 10 may under-represent the true throw on Qfo1 as the hanging wall is mantled with Qfi fan deposits. Along each profile black arrow indicates location of fault interpreted from lidar data. Profile locations are shown on Figure 9.

ing soil observations when considering cosmogenic exposure ages for alluvial surfaces. Additionally, the work reinforces the notion that slip rates on central Basin and Range faults are generally similar and consistent with similarities in alluvial fan geomorphology.

Acknowledgements

This work was partially funded by the U.S. Department of Energy (DOE) Geothermal Technologies Program under grant award DE-EE0009254. We gratefully acknowledge the University of Otago sabbatical leave program for partial support of Stirling during his stay in Reno. The University of Otago and the Nevada Bureau of Mines and Geology supported the cosmogenic dating costs. We thank Sylvia Nicovich, an anonymous reviewer, and Seismica editor Randolph Williams for insightful comments that improved the paper. Finally, we thank the participants of the 2024 Friends of the Pleistocene annual field trip early in this work for fruitful discussions and Jerry Annis of Buffalo Valley for land access, backhoe services, and ranch water.

Data and code availability

All data used in this study are contained in the manuscript and electronic supplement including soil descriptions, ^{36}Cl Depth profile data, ^{10}Be surface exposure data, geochemistry and input data to the CRONUScalc Matlab program, ^{10}Be production rate plots, and photographs of sampled boulders. 36Cl Depth profile model used in our analyses based on Marrero et al. (2016), CRONUScalc program available at https://bitbucket.org/cronusearth/cronus-calc/src/master/. CRONUScalc Matlab program used in 10Be exposure age modeling is available at https://hess.ess.washington.edu.

Competing interests

The authors have no competing interests

References

Adams, K. D. and Wesnousky, S. G. The Lake Lahontan highstand: age, surficial characteristics, soil development, and regional shoreline correlation. *Geomorphology*, 30(4):357–392, Dec. 1999. doi: 10.1016/s0169-555x(99)00031-8.

Adams, K. D., Goebel, T., Graf, K., Smith, G. M., Camp, A. J., Briggs, R. W., and Rhode, D. Late Pleistocene and Early Holocene lake-level fluctuations in the Lahontan Basin, Nevada: Implications for the distribution of archaeological sites. *Geoarchaeology*, 23 (5):608–643, Aug. 2008. doi: 10.1002/gea.20237.

Angster, S., Wesnousky, S., Figueiredo, P., Owen, L., and Hammer, S. Late Quaternary slip rates for faults of the central Walker Lane (Nevada, USA): Spatiotemporal strain release in a strike-slip fault system. *Geosphere*, 15(5), 2019. doi: 10.1130/GES02088.1.

Ayling, B., Faulds, J., Morales Rivera, A., Koehler, R., Kreemer, C., Mlawsky, E., Coolbaugh, M., Micander, R., DePolo, C., Kraal, K., Wagoner, N., Siler, D., DeAngelo, J., Glen, J., Peacock, J., Batir, J., Gentry, E., Berti, C., Lifton, Z., Clark, A., Kirby, S., Hardwick, C., and Kleber, E. INGENIOUS - Great Basin Regional Dataset Compilation, 2022. doi: 10.15121/1881483.

Bell, J., Caskey, S., Ramelli, A., and Guerrieri, L. Pattern and Rates of Faulting in the Central Nevada Seismic Belt, and Paleoseismic Evidence for Prior Beltlike Behavior. *Bulletin of the Seismological Society of America*, 94(4):1229–1254, Aug. 2004. doi: 10.1785/012003226.

Bormann, J., Surpless, B., Caffee, M., and Wesnousky, S. Holocene earthquakes and late Pleistocene slip-rate estimates on the Wassuk Range fault zone, Nevada. *Bulletin of the Seismological Association of America*, 102(4), 2012. doi: 10.1785/0120110287.

Burgess, Q. and Faulds, J. Characterizing a potential hidden geothermal system in Buffalo Valley, north-central Nevada. In *Abstracts and program, Geothermal Rising conference*, Reno, NV, 2023.

Eppes, M., McDonald, E., and McFadden, L. Soil geomorphological studies in the Mojave Desert: Impacts of Quaternary tectonics, climate, and rock type on soils, landscapes, and plant-community ecology. In Easterbrook, D., editor, *Quaternary Geology of the United States: International Union for Quaternary Research 2003 Field Guide Volume*, page 105–122. The Desert Research Institute, Reno, Nevada, 2003.

Faulds, J., Hinz, N., Coolbaugh, M., and Shevenell, L. The Nevada Play Fairway Project: Review of highly prospective areas for new discoveries of potentially viable geothermal systems in the Great Basin, western USA. *Geothermal Resources Council Transactions*, 40, GRC ID 1032368, 2016.

Faulds, J., Coolbaugh, M., and Hinz, N. Inventory of structural settings for active geothermal systems and late Miocene (8 MA) to Quaternary epithermal mineral deposits in the Basin and Range Province of Nevada. *Nevada Bureau of Mines and Geology Report*, 58:26, 2021.

Figueiredo, P., Wesnousky, S., and Owen, L. Late Pleistocene and Holocene paleoseismology and deformation rates of the Pleasant Valley fault (Nevada, USA). *Seismological Research Letters*, 94(2B):1029–1314, Mar. 2023. doi: 10.1785/0220230054.

Figueiredo, P., Wesnousky, S., Owen, L., Koehler, R., Stirling, M., Figueiredo, P., Reedy, T., Reheis, M., and Burgess, Q. Preliminary paleoseismic results from studies along the Pleasant Valley fault. *In*, 2024. https://fop.cascadiageo.org/pacific_cell/2024/2024_pac_cell_FOP_guidebook.pdf.

Hammond, W. C., Blewitt, G., and Kreemer, C. Steady contemporary deformation of the central Basin and Range Province, western United States. *Journal of Geophysical Research: Solid Earth*, 119(6), 2014. doi: 10.1002/2014jb011145.

Hanks, T. C. and Kanamori, H. A moment magnitude scale. *Journal of Geophysical Research: Solid Earth*, 84(B5):2348–2350, May 1979. doi: 10.1029/jb084ib05p02348.

Harden, D. R., Biggar, N. E., and Gillam, M. L. *Quaternary deposits and soils in and around Spanish Valley, Utah*, page 43–64. Geological Society of America, 1985. doi: 10.1130/spe203-p43.

Hatem, A. E., Collett, C. M., Briggs, R. W., Gold, R. D., Angster, S. J., Field, E. H., Powers, P. M., Anderson, M., Ben-Horin, J. Y., Dawson, T., DeLong, S., DuRoss, C., Jobe, J. T., Kleber, E., Knudsen, K. L., Koehler, R., Koning, D., Lifton, Z., Madin, I., Mauch, J., Pearthree, P., Pollitz, F., Scharer, K., Sherrod, B., Stickney, M., Wittke, S., and Zachariasen, J. Simplifying complex fault data for systems-level analysis: Earthquake geology inputs for U.S. NSHM 2023. *Scientific Data*, 9(1), Aug. 2022a. doi: 10.1038/s41597-022-01609-7.

Hatem, A. E., Reitman, N. G., Briggs, R. W., Gold, R. D., Thompson Jobe, J. A., and Burgette, R. J. Western U.S. Geologic Deformation Model for Use in the U.S. National Seismic Hazard Model 2023. *Seismological Research Letters*, 93(6), 2022b. doi: 10.1785/0220220154.

Koehler, R. D. and Wesnousky, S. G. Late Pleistocene regional extension rate derived from earthquake geology of late Quaternary faults across the Great Basin, Nevada, between 38.5 N and 40 N latitude. *Geological Society of America Bulletin*, 123(3-4): 631–650, 2011. doi: 10.1130/b30111.1.

Machette, M. N. *Calcic soils of the southwestern United States*, page 1–22. Geological Society of America, 1985. doi: 10.1130/spe203-p1.

Machette, M. N., Haller, K. M., Ruleman, C. A., Mahan, S., and Okumura, K. *Geologic evidence for late quaternary movement on the Clan Alpine Fault, west-central Nevada — Trench logs, scarp profiles, location maps, and sample and soil descriptions*. 2005. doi: 10.3133/sim2891.

Marrero, S. M., Phillips, F. M., Borchers, B., Lifton, N., Aumer, R., and Balco, G. Cosmogenic nuclide systematics and the CRONUScalc program. *Quaternary Geochronology*, 31:160–187, Feb. 2016. doi: 10.1016/j.quageo.2015.09.005.

Mifflin, M. and Wheat, M. Pluvial lakes and estimated pluvial climates of Nevada. *Nevada Bureau of Mines and Geology Bulletin*, 94(57), 1979.

Muller, S., Ferguson, H., and Roberts, R. Geology of the Mount Tobin quadrangle, Nevada. *U.S. Geological Survey, Geologic Quadrangle Map GQ-7*, 1(125), 1951.

Personius, S. F., Briggs, R. W., Maharrey, J. Z., Angster, S. J., and Mahan, S. A. A paleoseismic transect across the northwestern Basin and Range Province, northwestern Nevada and northeastern California, USA. *Geosphere*, 13(3):782–810, May 2017. doi: 10.1130/ges01380.1.

Petersen, M. D., Shumway, A. M., Powers, P. M., Field, E. H., Moschetti, M. P., Jaiswal, K. S., Milner, K. R., Rezaeian, S., Frankel, A. D., Llenos, A. L., Michael, A. J., Altekruse, J. M., Ahdi, S. K., Withers, K. B., Mueller, C. S., Zeng, Y., Chase, R. E., Salditch, L. M., Luco, N., Rukstales, K. S., Herrick, J. A., Girot, D. L., Aagaard, B. T., Bender, A. M., Blanpied, M. L., Briggs, R. W., Boyd, O. S., Clayton, B. S., DuRoss, C. B., Evans, E. L., Haeussler, P. J., Hatem, A. E., Haynie, K. L., Hearn, E. H., Johnson, K. M., Kortum, Z. A., Kwong, N. S., Makdisi, A. J., Mason, H. B., McNamara, D. E., McPhillips, D. F., Okubo, P. G., Page, M. T., Pollitz, F. F., Rubinstein, J. L., Shaw, B. E., Shen, Z., Shiro, B. R., Smith, J. A., Stephenson, W. J., Thompson, E. M., Thompson Jobe, J. A., Wirth, E. A., and Witter, R. C. The 2023 US 50-State National Seismic Hazard Model: Overview and implications. *Earthquake Spectra*, 40(1):5–88, Feb. 2024. doi: 10.1177/87552930231215428.

Redwine, J. R., Burke, R., Reheis, M., Bowers, R., Bright, J., Kaufman, D., and Forester*, R. *Middle and late Pleistocene pluvial history of Newark Valley, central Nevada, USA*, page 357–397. Geological Society of America, Aug. 2021. doi: 10.1130/2019.2536(18).

Reheis, M. *Extent of Pleistocene lakes in the western Great Basin*. 1999. doi: 10.3133/mf2323.

Stirling, M., Fitzgerald, M., Shaw, B., and Ross, C. New Magnitude–Area Scaling Relations for the New Zealand National Seismic Hazard Model 2022. *Bulletin of the Seismological Society of America*, 114(1):137–149, Dec. 2023. doi: 10.1785/0120230114.

USGS. Geoscience Data Acquisition for Western Nevada (GeoDAWN) project, 3D Elevation Program (3DEP). *DOE Geothermal Technologies Office*, 2023. https://www.usgs.gov/3d-elevation-program.

Valentini, A., DuRoss, C. B., Field, E. H., Gold, R. D., Briggs, R. W., Visini, F., and Pace, B. Relaxing Segmentation on the Wasatch Fault Zone: Impact on Seismic Hazard. *Bulletin of the Seismological Society of America*, 110(1):83–109, Nov. 2019. doi: 10.1785/0120190088.

Wallace, R. E., Bonilla, M. G., and Villalobos, H. A. *Faulting related to the 1915 earthquakes in Pleasant Valley, Nevada*. 1984. doi: 10.3133/pp1274ab.

Wesnousky, S. G., Barron, A. D., Briggs, R. W., Caskey, S. J., Kumar, S., and Owen, L. Paleoseismic transect across the northern Great Basin. *Journal of Geophysical Research: Solid Earth*, 110 (B5), May 2005. doi: 10.1029/2004jb003283.